



Contents lists available at ScienceDirect

## Dyes and Pigments

journal homepage: <http://www.elsevier.com/locate/dyepig>

# AEE-active conjugated polymers based on di (naphthalen-2-yl)-1,2-diphenylethene for sensitive fluorescence detection of picric acid

Yangpeng Zhuang<sup>a,1</sup>, Jinya Yao<sup>a,1</sup>, Zeyan Zhuang<sup>b</sup>, Chunjun Ni<sup>a</sup>, Hongming Yao<sup>a</sup>,  
Deliang Su<sup>a</sup>, Jian Zhou<sup>a,\*</sup>, Zujin Zhao<sup>b,\*\*</sup>

<sup>a</sup> College of Material, Chemistry and Chemical Engineering, Hangzhou Normal University, Hangzhou, 310036, China

<sup>b</sup> State Key Laboratory of Luminescent Materials and Devices, Key Laboratory of Luminescence from Molecular Aggregates of Guangdong Province, South China University of Technology, Guangzhou, 510640, China

## ARTICLE INFO

## Keywords:

Aggregation-enhanced emission  
Fluorescence detection  
Conjugated polymers  
di(naphthalen-2-yl)-1,2-diphenylethene  
Picric acid

## ABSTRACT

Picric acid (PA) is an archetypal explosive material that possesses low safety coefficient and high detonation velocity. The development of reliable and effective sensors for PA using PL spectroscopy methods is practically significant. Among various PL sensors, conjugated polymers have emerged as a class of fascinating candidates for the detection of PA due to the “molecular wire” sensing mechanism. In this work, we synthesized and characterized two new di (naphthalen-2-yl)-1,2-diphenylethene (DNDPE)-based conjugated polymers with different conjugation degree and hydrophilicity. They show good solubility, aggregation-enhanced emission (AEE) feature and high photostability. Both polymers exhibit sensitive fluorescence quenching by PA, and the KSV at the initial stage of the Stern–Volmer plots is up to  $9.8 \times 10^5 \text{ M}^{-1}$ . In addition, after exposure to UV light, these polymers still could effectively detect the PA in water. They also could on-site detect PA with high sensitivity by preparing the polymer-immobilized fluorescent test strips. The results demonstrate that these new DNDPE-based conjugated polymeric sensors could be good candidates for the sensitive detection of PA.

## 1. Introduction

The detection of explosive materials is crucial for security and stability of the society. The arising global terrorism has required the detection methods for explosives should be sensitive and convenient. So far, many explosives detection methods have been proposed, such as gas chromatography, mass spectrometry, surface-enhanced Raman spectroscopy, ion mobility spectrometry, photoluminescence (PL) spectroscopy and so on [1]. Among these mentioned methods, the PL spectroscopy methods have attracted increasing attention owing to their remarkable sensitivity, rapid response, convenience and low cost [2].

Picric acid (PA) is an archetypal kind of explosive materials that possesses low safety coefficient and high detonation velocity. Due to the good water solubility of PA, it is prone to contaminate soil and groundwater when widely applied in dyes or pesticide industries. At low concentration, it can give rise to human health disorders including

anemia, anaphylaxis and potential destructions to liver, kidney and respiratory system [3]. Therefore, the development of reliable and effective sensors for PA using PL spectroscopy methods is practically significant. Currently, much attention has been paid on various PL sensors based on quantum dots [4], metal-organic frameworks [5], conjugated polymers [6], nanosheets [7], etc. Among them, conjugated polymers have emerged as a class of fascinating candidates for the detection of PA due to the “molecular wire” sensing mechanism. When the photo-induced electron in the conjugated polymers delocalizes along the chains and transfers from electron-rich conjugated polymers to electron-deficient PA, the fluorescence of polymers could be quenched efficiently [8]. However, to attain ultrasensitivity and minimize the sensor's content for practical applications, it is still essential and meaningful to further develop novel conjugated polymeric sensors with special molecular structures.

In our previous researches, we developed tailor-made naphthalene-

\* Corresponding author.

\*\* Corresponding author.

E-mail addresses: [zhoujian@hznu.edu.cn](mailto:zhoujian@hznu.edu.cn) (J. Zhou), [mszjzhao@scut.edu.cn](mailto:mszjzhao@scut.edu.cn) (Z. Zhao).

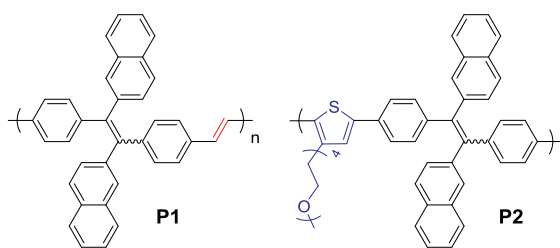
<sup>1</sup> These authors contributed equally to this work.

<https://doi.org/10.1016/j.dyepig.2019.108041>

Received 18 September 2019; Received in revised form 9 November 2019; Accepted 11 November 2019

Available online 14 November 2019

0143-7208/© 2019 Elsevier Ltd. All rights reserved.



**Scheme 1.** Molecular structure of DNDPE-based conjugated polymers.

substituted ethenes that held prominent aggregation-induced emission (AIE) property [9]. Based on the unit, di(naphthalen-2-yl)-1,2-diphenylethene (DNDPE), a series of new conjugated polymers were further synthesized [10]. In these polymers, the twisted conformation of DNDPE constructs the “cage” structure of the polymer chains, which could effectively capture the PA in solution, thus facilitating the photo-induced electron transfer (PET) and strengthening the fluorescence quenching efficiency. With the “cage” idea in mind, we recently developed two new DNDPE-based conjugated polymers with different conjugation degree and hydrophilicity. Both of them show aggregation-enhanced emission (AEE) feature and perform efficiently in the detection of PA.

## 2. Experimental

### 2.1. General

THF was distilled from sodium benzophenone ketyl under dry nitrogen immediately prior to use. Chemicals and reagents were purchased from Aldrich and J&K Scientific Ltd., and used as received without further purification.  $^1\text{H}$  and  $^{13}\text{C}$  NMR spectra were measured on a Bruker AV 500 spectrometer in deuterated chloroform using tetramethylsilane (TMS;  $\delta = 0$ ) as internal reference. UV-vis absorption spectra were measured on a Shimadzu UV-2600 spectrophotometer. Photoluminescence was recorded on a PerkinElmer LS 55 spectrofluorometer. Mass spectra were recorded on an Agilent 1290 Infinity LC/6530 Q-TOF MS. The number ( $M_n$ ) and weight average ( $M_w$ ) molecular weights and polydispersity indices (PDI or  $M_w/M_n$ ) of the polymers were estimated by a Waters Associates gel permeation chromatography (GPC 2414) system equipped with RI and UV detectors. The ground-state geometries were optimized using the density functional theory (DFT) method with B3LYP hybrid functional at the basis set level of 6-31G(d). All the calculations were performed using Gaussian 09 package.

### 2.2. Explosive detection

A solution of picric acid (PA) in ethanol with a concentration of  $0.1 \text{ mg mL}^{-1}$  was prepared by dissolving an appropriate amount of PA in ethanol. Photoluminescence titration was carried out by adding aliquots of PA solution into solutions of P1 and P2 in THF/water mixtures (P1:  $f_w = 90 \text{ vol\%}$ ; P2:  $f_w = 80 \text{ vol\%}$ ).

## 3. Results and discussion

### 3.1. Synthesis

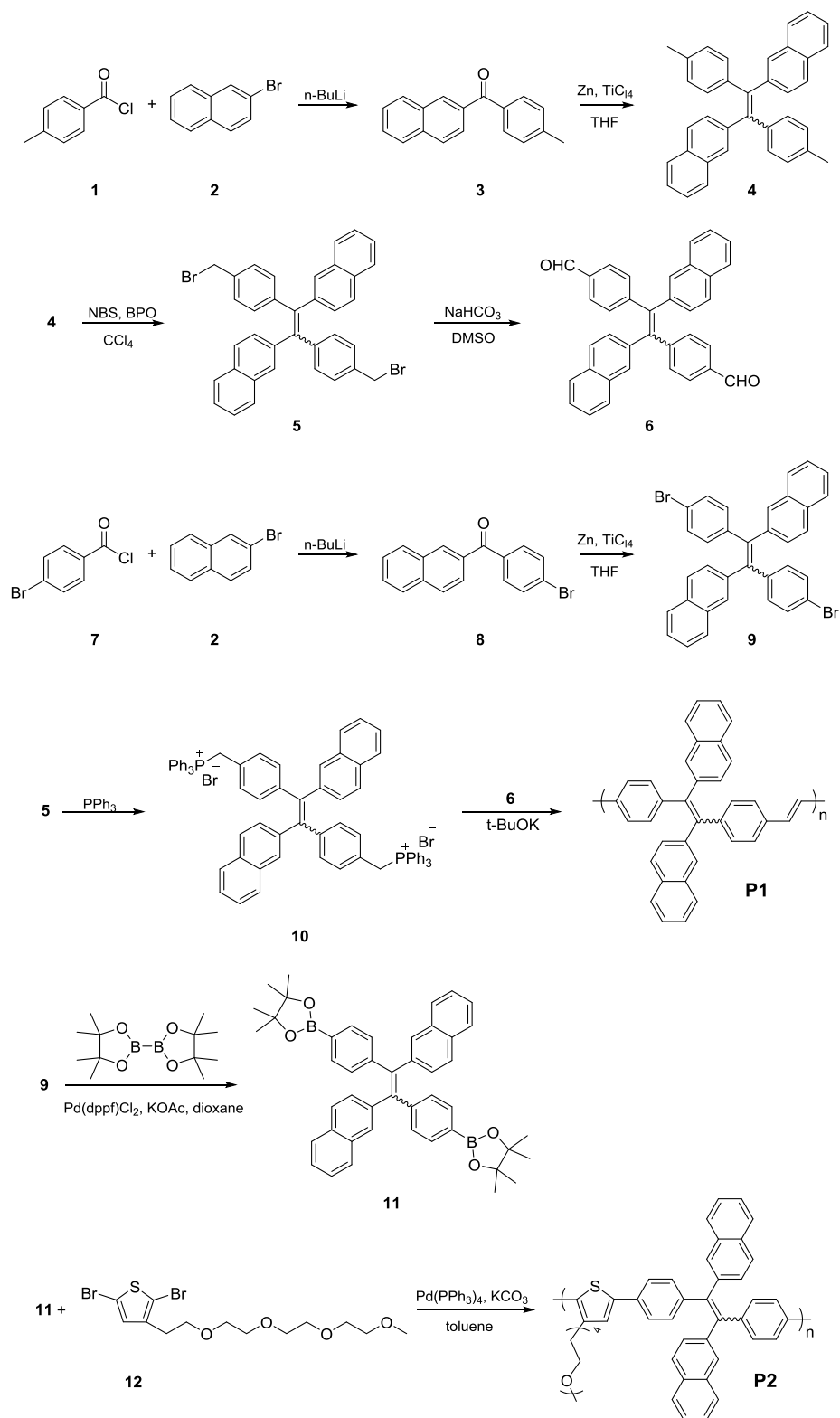
**Scheme 1** shows the molecular structures of the DNDPE-based conjugated polymers **P1** and **P2**. The detailed synthetic routes and characterization for monomers and polymers are depicted in **Scheme 2**. Briefly, the Wittig reaction of 4,4'-(1,2-di(naphthalen-2-yl)ethene-1,2-diyl)dibenzaldehyde and corresponding phosphonium salt in the presence of potassium *tert*-butoxide afforded **P1** in 35% yield. The palladium-

catalyzed Suzuki coupling reaction of 13-(thiophen-3-yl)-2,5,8,11-tetraoxatridecane with 1,2-di(naphthalen-2-yl)-1,2-bis(4-(4,4,5,5-tetramethyl-1,3,2-dioxaborolan-2-yl)phenyl)ethene produced **P2** in 59% yield. The use of flexible long-chain ether groups enhances the hydrophilicity of **P2** and impels the formation of intumescent and stable aggregates. The molecular weight ( $M_w$ ) values of polymers were analyzed by the GPC experiment using polystyrene as an internal standard. The  $M_w$  and polydispersity (PDI) of **P1** are  $20669 \text{ g mol}^{-1}$  and 1.64, respectively. In the presence of long-chain ether groups, the  $M_w$  of **P2** is increased to  $50576 \text{ g mol}^{-1}$  and the PDI is still around 1.62. The prepared **P1** and **P2** were readily soluble in common organic solvents like  $\text{CHCl}_3$ , toluene, THF and DMSO.

**Naphthalen-2-yl(*p*-tolyl)methanone (3):** A solution of *n*-BuLi (9.4 mL, 14.49 mmol) in *n*-hexane was added dropwise to a solution of 2-bromonaphthalene (3 g, 14.49 mmol) in dry THF (150 mL) under  $\text{N}_2$  at  $-78^\circ\text{C}$ . After stirring for 1 h, the solution was transferred to excess *p*-toluoyl chloride (3.36 g, 21.73 mmol) in dry THF (30 mL). The resulting mixture was kept at  $-78^\circ\text{C}$  for 30 min. The mixture was then warmed to room temperature and stirred overnight. Then  $\text{K}_2\text{CO}_3$  solution (1 M, 5 mL) was added to the mixture. The mixture was extracted with ethyl acetate by three times. The combined organic layers were washed with water, and dried over anhydrous  $\text{MgSO}_4$ . After filtration and solvent evaporation, the residue was purified by silica-gel column chromatography using hexane/dichloromethane as eluent. White solid of **3** was obtained in 26.7% yield.  $^1\text{H}$  NMR (500 MHz,  $\text{CDCl}_3$ ),  $\delta$  (TMS, ppm):  $\delta$  8.25 (s, 1H), 7.97–7.89 (m, 4H), 7.78 (d, 2H,  $J = 8.1 \text{ Hz}$ ), 7.64–7.53 (m, 2H), 7.32 (d, 2H,  $J = 7.9 \text{ Hz}$ ), 2.47 (s, 3H).  $^{13}\text{C}$  NMR (126 MHz,  $\text{CDCl}_3$ ): 195.4, 142.1, 134.1, 131.2, 130.5, 129.3, 128.3, 128.0, 127.2, 127.1, 126.8, 125.7, 124.8, 20.6. HRMS:  $m/z$  247.1102 ( $[\text{M}+\text{H}]^+$ , calcd for  $\text{C}_{18}\text{H}_{15}\text{O}$  247.1123).

**1,2-Bis(4-bromophenyl)-1,2-di(naphthalen-2-yl)ethene (4):** Into a 250 mL two-necked round-bottom flask with a reflux condenser were placed **3** (1.5 g, 6.09 mmol), zinc dust (4.78 g, 79.17 mmol). The flask was evacuated under vacuum and flushed with dry  $\text{N}_2$  three times. Dry THF (100 mL) was then added. The mixture was cooled to  $-78^\circ\text{C}$  and  $\text{TiCl}_4$  (1.39 g, 7.31 mmol) was added dropwise by a syringe. After stirred for 0.5 h, the reaction mixture was warmed to room temperature and then heated to reflux for 12 h. The mixture was cooled to room temperature and poured into water, and extracted with dichloromethane by three times. The combined organic layers were washed with saturated brine solution and water, and dried over anhydrous  $\text{MgSO}_4$ . After filtration and solvent evaporation, the residue was purified by silica-gel column chromatography using hexane/dichloromethane as eluent. White solid of **4** was obtained in 52% yield.  $^1\text{H}$  NMR (500 MHz,  $\text{CDCl}_3$ ),  $\delta$  (TMS, ppm): 7.73 (d, 1H,  $J = 7.7 \text{ Hz}$ ), 7.65 (d, 1H,  $J = 7.9 \text{ Hz}$ ), 7.61–7.51 (m, 5H), 7.47 (d, 1H,  $J = 8.5 \text{ Hz}$ ), 7.41–7.29 (m, 4H), 7.22–7.16 (m, 2H), 6.99–6.92 (m, 6H), 6.85 (d, 2H,  $J = 7.9 \text{ Hz}$ ), 2.28 (s, 3H), 2.21 (s, 3H).  $^{13}\text{C}$  NMR (126 MHz,  $\text{CDCl}_3$ ): 142.0, 141.7, 141.2, 140.9, 140.8, 136.2, 133.3, 132.1, 131.5, 131.4, 130.5, 130.4, 129.8, 128.5, 128.1, 128.0, 127.5, 127.0, 125.7, 21.2. HRMS:  $m/z$  461.2267 ( $[\text{M}+\text{H}]^+$ , calcd for  $\text{C}_{36}\text{H}_{29}$  461.2269).

**1,2-Bis(4-(bromomethyl)phenyl)-1,2-di(naphthalen-2-yl)ethene (5):** Into a 250 mL round-bottom flask with a reflux condenser were placed **4** (1.0 g, 2.17 mmol), NBS (0.97 g, 5.43 mmol), and BPO (52.6 mg, 0.217 mmol) followed by addition of 30 mL of  $\text{CCl}_4$ . After refluxed for 24 h, the mixture was cooled to room temperature and filtered, the solvent was evaporated under reduced pressure. The crude product was purified by silica-gel column chromatography using petroleum ether as eluent to give **5** as yellow solid in 53.2% yield.  $^1\text{H}$  NMR (500 MHz,  $\text{CDCl}_3$ ),  $\delta$  (TMS, ppm): 7.74 (d, 1H,  $J = 7.9 \text{ Hz}$ ), 7.67 (d, 1H,  $J = 7.8 \text{ Hz}$ ), 7.61–7.53 (m, 3H), 7.53–7.47 (m, 3H), 7.43–7.32 (m, 4H), 7.17–7.14 (m, 4H), 7.09–7.03 (m, 6H), 4.44 (s, 2H), 4.37 (s, 2H).  $^{13}\text{C}$  NMR (126 MHz,  $\text{CDCl}_3$ ): 143.96, 143.81, 141.18, 140.88, 133.18, 132.25, 131.91, 130.64, 129.42, 128.63, 128.06, 127.56, 127.24, 125.96, 125.92, 33.55. HRMS:  $m/z$  618.0415 ( $\text{M}^+$  calcd for  $\text{C}_{36}\text{H}_{26}\text{Br}_2$  618.0381).



**Scheme 2.** Molecular structures and synthetic routes to DNDPE-based conjugated polymers P1 and P2.

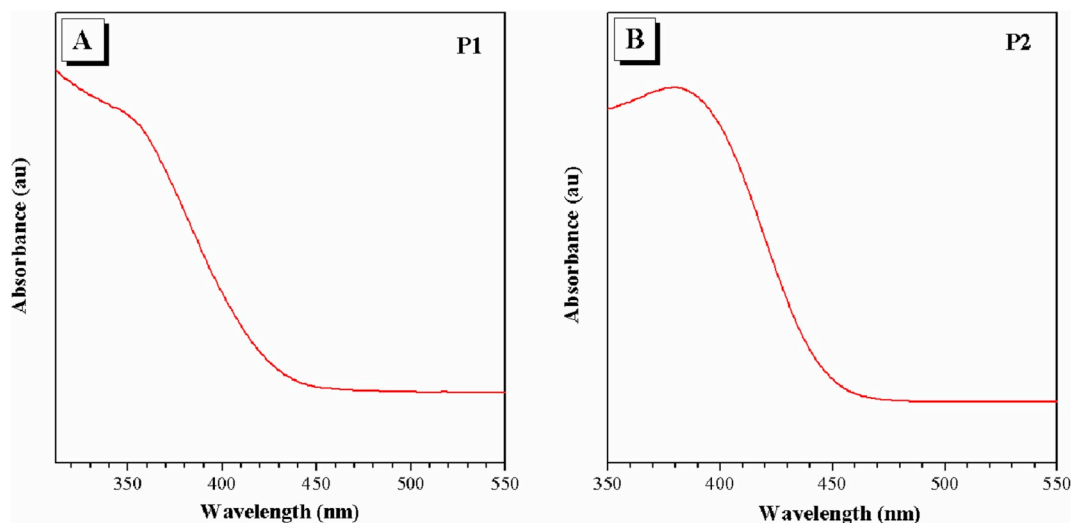


Fig. 1. Absorption spectra of THF solutions of P1 (A) and P2 (B). Solution concentration:  $10^{-5}$  M.

#### 4,4'-(1,2-Di(naphthalen-2-yl)ethene-1,2-diyl)dibenzaldehyde

(6):  $\text{NaHCO}_3$  (0.27 g, 3.24 mmol) was added to a stirred solution of **5** (0.5 g, 0.809 mmol) in DMSO (3.7 mL) and the mixture was stirred at  $95^\circ\text{C}$  for 4 h. The mixture was cooled back to room temperature, diluted with water, extracted with dichloromethane by three times. The organic layer was dried over anhydrous  $\text{MgSO}_4$ . After filtration and solvent evaporation, the crude product was purified by silica-gel column chromatography and **6** was obtained as a yellow solid in 37.3% yield.  $^1\text{H}$  NMR (500 MHz,  $\text{CDCl}_3$ ),  $\delta$  (TMS, ppm): 9.94 (s, 2H), 7.70 (d, 2H,  $J = 8.0$  Hz), 7.66 (d, 4H,  $J = 8.3$  Hz), 7.58–7.35 (m, 12H), 7.27 (s, 2H), 7.16 (dd, 2H,  $J = 8.5, 1.7$  Hz).  $^{13}\text{C}$  NMR (126 MHz,  $\text{CDCl}_3$ ): 191.76, 149.73, 142.07, 139.78, 134.70, 133.12, 132.45, 132.08, 130.80, 129.36, 128.88, 128.02, 127.76, 127.63, 126.50, 126.30. HRMS:  $m/z$  488.1781 ( $\text{M}^+$ , calcd for  $\text{C}_{36}\text{H}_{24}\text{O}_2$  488.1776).

(4-Bromophenyl) (naphthalen-2-yl)methanone (**8**): A solution of  $n\text{-BuLi}$  (9.4 mL, 14.49 mmol) in  $n\text{-hexane}$  was added dropwise to a solution of 2-bromonaphthalene (3 g, 14.49 mmol) in dry THF (150 mL) under  $\text{N}_2$  at  $-78^\circ\text{C}$ . After stirring for 1 h, the solution was transferred to excess 4-bromobenzoyl chloride (4.77 g, 21.73 mmol) in dry THF (30 mL). The resulting mixture was kept at  $-78^\circ\text{C}$  for 30 min. The mixture was then warmed to room temperature and stirred overnight. Then  $\text{K}_2\text{CO}_3$  solution (1 M, 5 mL) was added to the mixture. The mixture was extracted with ethyl acetate by three times. The combined organic layers were washed with water, and dried over anhydrous  $\text{MgSO}_4$ . After filtration and solvent evaporation, the residue was purified by silica-gel column chromatography using hexane/dichloromethane as eluent. White solid of **8** was obtained in 22.7% yield.  $^1\text{H}$  NMR (500 MHz,  $\text{CDCl}_3$ ),  $\delta$  (TMS, ppm): 8.22 (s, 1H), 7.95–7.87 (m, 4H), 7.72 (d, 2H,  $J = 8.5$  Hz), 7.67–7.58 (m, 3H), 7.57–7.53 (m, 1H).  $^{13}\text{C}$  NMR (126 MHz,  $\text{CDCl}_3$ ),  $\delta$  (TMS, ppm): 195.63, 136.63, 135.36, 134.42, 132.24, 131.82, 131.69, 131.62, 129.44, 128.53, 128.50, 127.88, 127.47, 126.97, 125.59. HRMS:  $m/z$  311.0071 ( $[\text{M}+\text{H}]^+$ , calcd for  $\text{C}_{17}\text{H}_{12}\text{BrO}$  311.0072).

1,2-Bis(4-bromophenyl)-1,2-di(naphthalen-2-yl)ethene (**9**): Into a 250 mL two-necked round-bottom flask with a reflux condenser were placed **8** (1.5 g, 4.8 mmol), zinc dust (3.76 g, 57.8 mmol). The flask was evacuated under vacuum and flushed with dry nitrogen three times. 100 mL of dry THF was then added. The mixture was cooled to  $-78^\circ\text{C}$  and  $\text{TiCl}_4$  (1.09 g, 5.76 mmol) was added dropwise by a syringe. After stirred for 0.5 h, the reaction mixture was warmed to room temperature and then heated to reflux for 12 h. The mixture was cooled to room temperature and poured into water, and extracted with dichloromethane by three times. The combined organic layers were washed with

saturated brine solution and water, and dried over anhydrous  $\text{MgSO}_4$ . After filtration and solvent evaporation, the residue was purified by silica-gel column chromatography using hexane/dichloromethane as eluent. White solid of **9** was obtained in 49% yield.  $^1\text{H}$  NMR (500 MHz,  $\text{CDCl}_3$ ),  $\delta$  (TMS, ppm): 7.79 (d, 1H,  $J = 7.7$  Hz), 7.71 (d, 1H,  $J = 7.8$  Hz), 7.65 (dd, 2H,  $J = 7.9, 4.7$  Hz), 7.58 (d, 1H,  $J = 7.9$  Hz), 7.53 (d, 3H,  $J = 8.7$  Hz), 7.49–7.36 (m, 4H), 7.32 (d, 2H,  $J = 8.4$  Hz), 7.24–7.15 (m, 4H), 7.02–6.95 (m, 4H).  $^{13}\text{C}$  NMR (126 MHz,  $\text{CDCl}_3$ ),  $\delta$  (TMS, ppm): 142.58, 140.63, 140.51, 133.16, 131.23, 133.11, 130.64, 130.59, 129.24, 128.06, 127.54, 127.51, 127.36, 126.11, 125.96, 121.00. HRMS:  $m/z$  590.0072 ( $\text{M}^+$ , calcd for  $\text{C}_{34}\text{H}_{22}\text{Br}_2$  590.0068).

((1,2-Di(naphthalen-2-yl)ethene-1,2-diyl)bis(4,1-phenylene)) bis(methylene)bis(triphenylphosphonium) bromide (**10**): Into a 100 mL round-bottom flask with a reflux condenser were placed **5** (0.5 g, 0.81 mmol) and  $\text{PPh}_3$  (0.85 g, 3.24 mmol). 30 mL of DMF was then added. After heated to  $100^\circ\text{C}$  for 24 h, the mixture was cooled to room temperature and poured into toluene. The precipitates were filtered and washed with toluene to give **10** as yellow solid in 53% yield.  $^1\text{H}$  NMR (500 MHz,  $\text{CDCl}_3$ ),  $\delta$  (TMS, ppm): 7.77–7.31 (m, 44H), 6.99 (d, 2H,  $J = 8.0$  Hz), 6.81 (s, 4H), 6.73 (s, 2H), 2.42 (s, 4H). HRMS:  $m/z$  1061.3049 ( $[\text{M} - \text{Br}]^+$ , calcd for  $[\text{C}_{72}\text{H}_{56}\text{P}_2\text{Br}]^+$  1061.3041).

1,2-Di(naphthalen-2-yl)-1,2-bis(4-(4,4,5,5-tetramethyl-1,3,2-dioxaborolan-2-yl)phenyl)ethene (**11**): **9** (1 g, 1.7 mmol), bis-(pinacolato)diborane (1.22 g, 4.8 mmol), KOAc (1.17 g, 11.9 mmol), and dioxane (30 mL) were mixed together in a 100 mL flask. After degassing,  $[\text{Pd}(\text{dppf})\text{Cl}_2]$  (0.24 g,  $\text{dppf} = 1,1'$ -bis(diphenylphosphanyl)ferrocene) was added. The reaction mixture was kept at  $100^\circ\text{C}$  for 24 h, and then cooled to room temperature. The organic solvent was distilled out, and the residual solid was dissolved in dichloromethane and washed with saturated brine solution. After drying with anhydrous  $\text{MgSO}_4$ , the solvent was distilled out. The crude product was purified by flash chromatography using dichloromethane as the eluent and then recrystallized in isopropanol to give **11** as white crystals (0.23 g, 20%).  $^1\text{H}$  NMR (500 MHz,  $\text{CDCl}_3$ ),  $\delta$  (TMS, ppm): 7.72 (d, 2H,  $J = 7.9$  Hz), 7.59–7.53 (m, 4H), 7.49 (d, 6H,  $J = 7.7$  Hz), 7.41–7.34 (m, 4H), 7.16 (dd, 2H,  $J = 8.4, 1.5$  Hz), 7.09 (d, 4H,  $J = 8.0$  Hz), 1.29 (s, 24H).  $^{13}\text{C}$  NMR (126 MHz,  $\text{CDCl}_3$ ),  $\delta$  (TMS, ppm): 145.68, 140.62, 140.10, 133.18, 132.10, 131.15, 129.91, 129.55, 128.47, 127.07, 126.46, 126.07, 124.66, 82.70, 82.65, 23.84. HRMS:  $m/z$  684.3579 ( $\text{M}^+$ , calcd for  $\text{C}_{46}\text{H}_{46}\text{B}_2\text{O}_4$  684.3582).

**P1**: To a three-necked, round-bottom flask was added **10** (50 mg, 0.044 mmol) in 3 mL of dry DMF under nitrogen in an ice-water bath. Potassium *tert*-butoxide (14.8 mg, 0.132 mmol) was then added under stirring. The intense orange solution was stirred at room temperature for

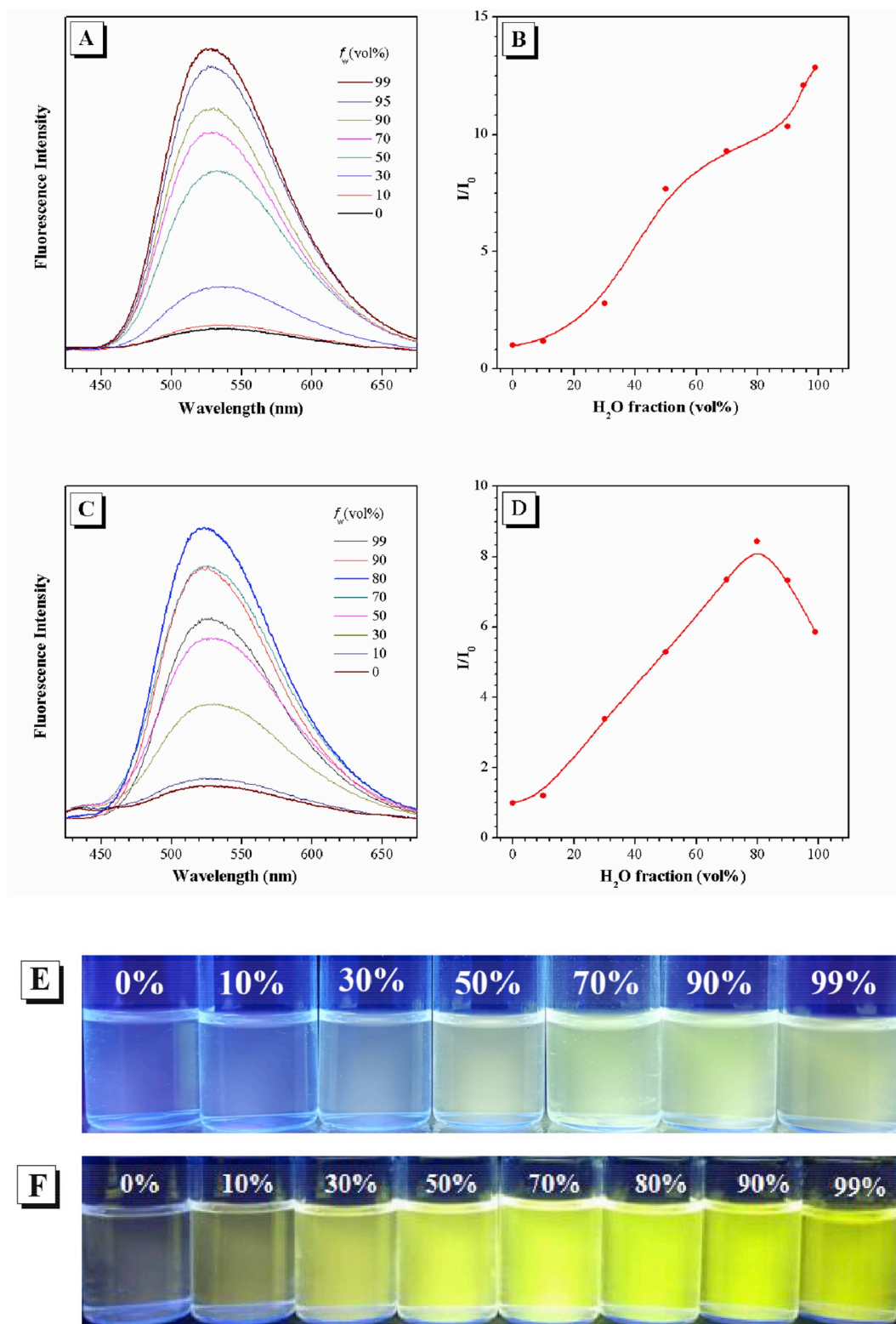
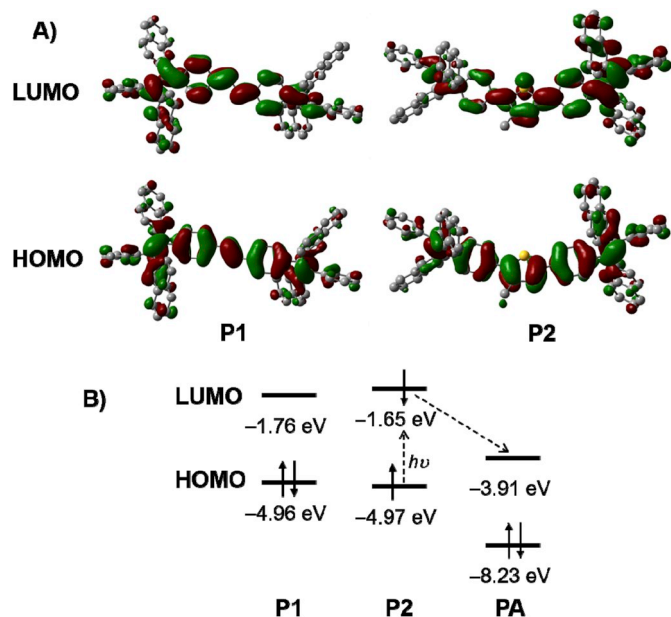


Fig. 2. (A and C) Fluorescence spectra of P1 and P2 in THF/water mixtures with different water fractions ( $f_w$ ), respectively. (B and D) Plots of  $I/I_0$  versus the compositions of the aqueous mixtures.  $I_0$  = fluorescence intensity in pure THF solution. E and F: photographs of P1 and P2 in THF/water mixtures with different  $f_w$ , taken under the illumination of a UV lamp (365 nm). Concentration: 10  $\mu$ M; excitation wavelength: 350 nm.

30 min, after which a solution of **6** (21.5 mg, 0.044 mmol) in 2 mL of dry DMF was added. The reaction mixture was stirred at room temperature overnight. The reaction mixture was poured into ice water and yellow precipitates were collected. The crude product was washed with cold

ethanol. The residue was dissolved in THF and added into 200 mL of petroleum ether. Yellow solid of **P1** was obtained in 35% yield. <sup>1</sup>H NMR (500 MHz, CDCl<sub>3</sub>),  $\delta$  (TMS, ppm): 7.70–7.38 (m, 10H), 7.31 (s, 2H), 7.28 (s, 2H), 7.13–7.03 (m, 4H), 6.99–6.93 (m, 2H), 6.91 (s, 2H), 6.80–6.69



**Fig. 3.** (A) Optimized conformations and calculated molecular orbital amplitude plots of HOMOs and LUMOs for the conjugated fragments M1 and M2 for **P1** and **P2**, respectively. (B) Calculated energy level diagram of M1, M2 and PA.

(m, 2H).  $M_n = 12603$ ; PDI ( $M_w/M_n$ ) = 1.64.

**P2:** To a mixture of **11** (170 mg, 0.25 mmol), **12** (75 mg, 0.25 mmol), Pd(PPh<sub>3</sub>)<sub>4</sub> (12 mg, 0.01 mmol) and K<sub>2</sub>CO<sub>3</sub> (276 mg, 2 mmol) in a 10 mL round-bottomed flask. A mixture of toluene (1 mL) and water (1 mL) was added to the flask, and the reaction vessel was degassed. The mixture was vigorously stirred at 90 °C for 24 h and then cooled to room temperature. After extraction with dichloromethane, the combined organic layers were washed successively with water and then dried over anhydrous MgSO<sub>4</sub>. The polymer was filtered and precipitated into methanol, and then dried under vacuum for 24 h to afford the neutral polymer **P2** as a yellow solid in 59% yield. <sup>1</sup>H NMR (500 MHz, CDCl<sub>3</sub>), δ (TMS, ppm): 7.68–7.44 (m, 9H), 7.29 (s, 6H), 7.03 (s, 8H), 3.60–3.43 (m, 14H), 3.24 (s, 3H), 2.95–2.66 (m, 2H).  $M_n = 31220$ , PDI ( $M_w/M_n$ ) = 1.621.

### 3.2. Optical property

**Fig. 1** shows the absorption spectra of **P1** and **P2** in dilute THF (10 μM). The absorption maximum of **P2** is located at 379 nm, while **P1** does not show obvious absorption peaks. The fluorescence spectra of **P1** and **P2** in dilute THF (10 μM) exhibit broad and weak peaks due to the random-coil configurations of the polymer, which partly restrict the intramolecular rotations and suppress the nonradiative decay [11]. With the gradual addition of water, a poor solvent for the polymers, into THF, the fluorescence intensity of the polymers progressively enhances. The strong emission peak of **P1** emerges at 529 nm, whose intensity rises by 14-fold from the isolated species in THF solution to the aggregates in 99% aqueous mixture (**Fig. 2A** and **B**). **P2** displays the emission peak at 523 nm in 80% aqueous mixture and decreases slightly at a higher water fraction ( $f_w$ ) in the THF/water mixture (>80%) (**Fig. 2C** and **D**). The photographs of **P1** and **P2** in THF/water mixtures with different water fractions are shown in **Fig. 2E** and **F**, taken under the UV lamp illumination at 365 nm. The enhancement in fluorescence intensity is thus caused by the aggregate formation, demonstrating the AEE feature.

### 3.3. Electronic structure and energy level

Theory calculations of the conjugated fragments of **P1** and **P2** using

the density functional theory (DFT) were carried out to study their electronic structures and energy levels. As shown in **Fig. 3**, the highest occupied molecular orbitals (HOMOs) and the lowest unoccupied molecular orbitals (LUMOs) occupy all the building blocks in conjugated fragments, demonstrating the good conjugation of the backbones. There are also electronic clouds of HOMOs and LUMOs located on the naphthalen-2-yl moiety in **P1** and **P2**, indicating that the rotation of naphthalen-2-yl groups could deactivate the excited states and result in weak PL emissions of polymers in solutions.

### 3.4. Explosive detection

To explore the potential use of **P1** and **P2** as fluorescent chemosensors for sensitive detection of PA, the aggregates of **P1** in THF/water mixtures ( $f_w = 90$  vol%) and **P2** in THF/water mixtures ( $f_w = 80$  vol%) were used as probes for detection, respectively. As shown in **Fig. 4A** and **B**, with the addition of PA to the aggregate suspension of **P1**, the fluorescence intensity is gradually quenched. The detection limit of PA is calculated to be 0.181 μM. At low concentrations of PA, the Stern–Volmer plot is linear and gives a quenching constant ( $K_{SV}$ ) of  $4.7 \times 10^4 \text{ M}^{-1}$ , which is higher than those ( $K_{SV} < 1.2 \times 10^4 \text{ M}^{-1}$ ) of the DNDPE-based conjugated polymers reported previously [10]. Similar quenching effect is also observed for **P2**. In addition, the aggregate suspension of **P2** can detect PA with extremely good sensitivity. The fluorescence intensity is rapidly quenched, even at 1.4 μM, with an increase of PA concentration. The  $K_{SV}$  for **P2** at the initial stage of the Stern–Volmer plots reaches to  $9.8 \times 10^5 \text{ M}^{-1}$  (**Fig. 4C** and **D**). These results reveal that **P2** is much more sensitive to PA than **P1**, which is probably owing to that the aggregates of **P2** can associate with more PA because of the existence of numerous cavities generated by the loose packing of **P2** with twisted molecular conformations and higher hydrophilicity. As to the quenching mechanism, the absorption spectrum of PA hardly overlaps with the emission spectra of **P1** and **P2** (**Fig. 5**), resulting in poor secondary inner filter effect (IFE) or fluorescence resonance energy transfer (FRET) efficiency, though some contribution of primary IFE cannot be ruled out [12]. Furthermore, the energy levels of HOMOs and LUMOs of the polymer fragments and PA are calculated. The LUMO energy level of PA is much lower than those of **P1** and **P2**, and is even close to the HOMO energy levels of **P1** and **P2**, revealing that excited state electron transfer from the LUMOs of **P1** and **P2** to the LUMO of PA is promoted upon photoexcitation (**Fig. 3**), which causes efficient PL quenching.

The photostability of **P1** and **P2** in THF/water mixtures was also tested. Under continuous exposure to UV light, the fluorescence intensity of **P1** in THF/water mixtures declines slowly at the beginning. After continuous radiation for 60 min, the fluorescence intensity at 518 nm shows a moderate decrease by 43% (**Fig. 6A** and **B**). **P2** displays similar photostability within 60 min (**Fig. 6C** and **D**). Even after continuous radiation for 24 h, **P2** in THF/water mixtures still retains the 13% fluorescence intensity. Furthermore, to check the PA sensing properties of polymers after exposure to UV light, fluorescence quenching titration experiments have been further performed by addition ethanol solutions of PA into the exposure samples (60 min radiation). The fluorescence quenching of ~43% for **P1** aggregates is observed upon exposure to UV light for 60 min, which is further immediately quenched by ~74% upon adding 10.65 μM PA solution (**Fig. 7A**). In the presence of the same amount of PA, however, the fluorescence of **P2** aggregates exposed to UV is quenched by ~58%, implying the cavities in **P2** aggregates are changed under UV light, which attenuate the interaction with PA molecule (**Fig. 7B**).

Considering the practical application in explosives detection, the instant surface sensing of PA by preparing fluorescent test strips was performed. Several pieces of Whatman filter paper were impregnated with a THF solution of **P1** (or **P2**) at a concentration of 0.1 mg mL<sup>-1</sup> and then dried. A solvent spot was also applied as a blank. Under the irradiation of 365 nm UV light, the discernible dark spots on the filter paper

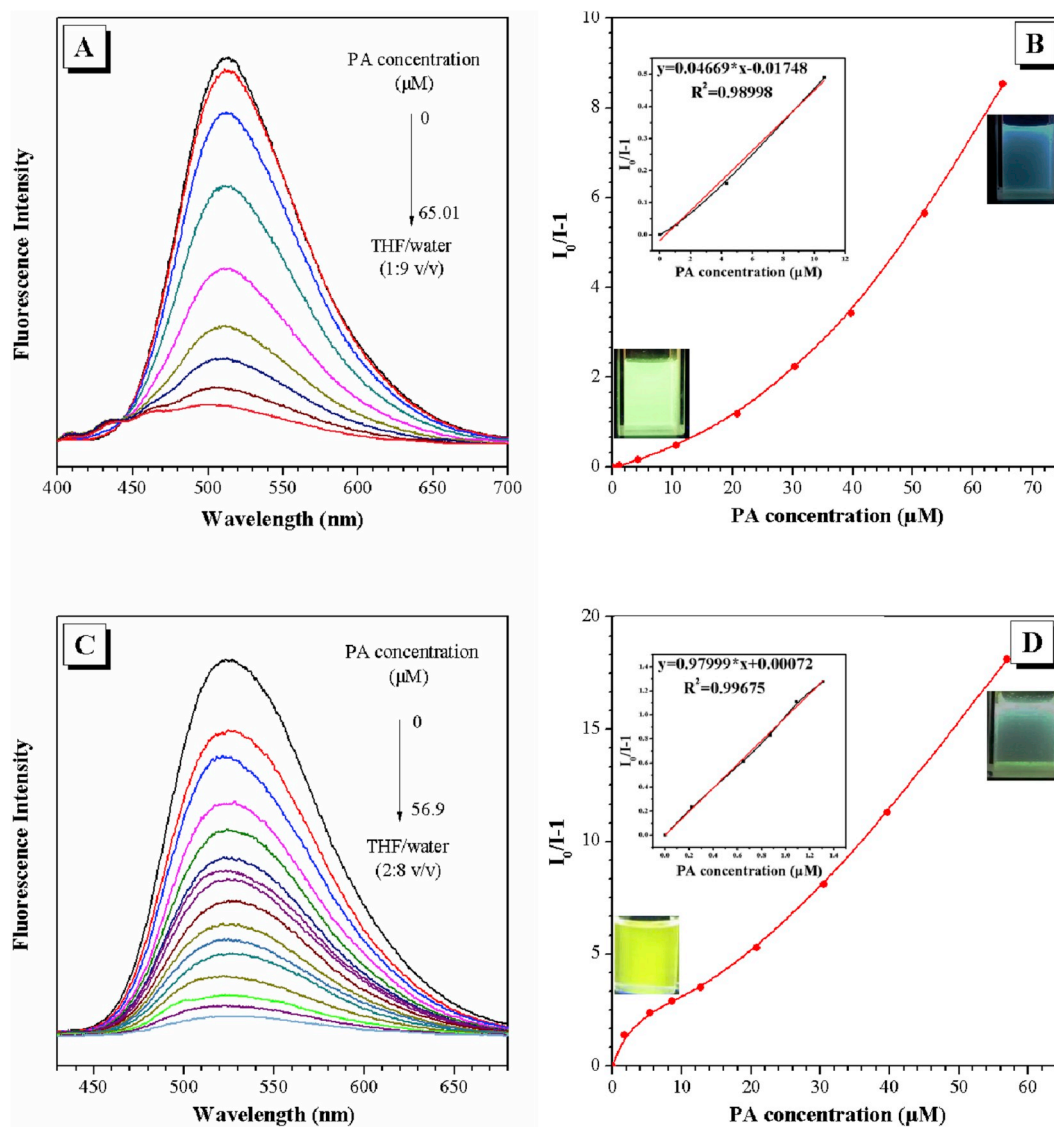


**Fig. 4.** (A and C) Fluorescence spectra of P1 and P2 in THF/water mixtures ( $f_w = 90$  vol%) containing different amounts of PA. (B and D) Plots of  $I_0/I-1$  value versus PA concentration in THF/water mixtures (P1:  $f_w = 90$  vol%; P2:  $f_w = 80$  vol%). Inset: photographs of P1 and P2 in THF/water mixtures with different PA concentration (P1: 0 and 65.01  $\mu\text{M}$ ; P2: 0 and 56.9  $\mu\text{M}$ ), taken under the illumination of a UV lamp (365 nm). Concentration: 0.53  $\mu\text{M}$  (P1), 0.21  $\mu\text{M}$  (P2); excitation wavelength: 350 nm.

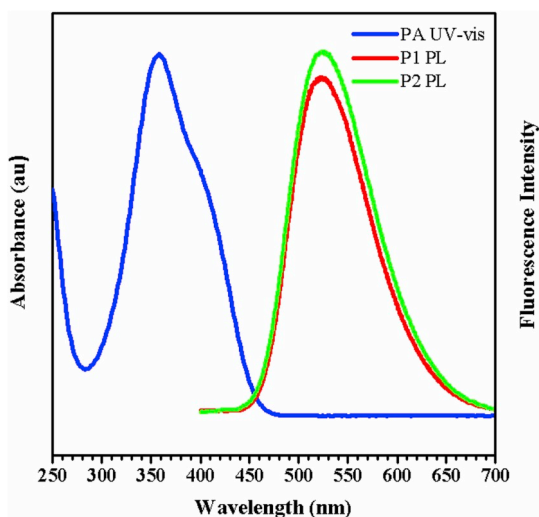


Fig. 5. Normalized absorption spectra of PA in ethanol solution and fluorescence spectra of P1 and P2 in THF/water mixtures ( $f_w = 90$  vol%).

were observed by adding 1  $\mu$ L of different concentrations of PA, indicating the fluorescence was quenched in varying degrees by PA (Fig. 8). The minimum amount of PA that can be detected by naked eye using P1-immobilized filter paper was found to be as low as 22.9 fg ( $10^{-10}$  M), while the detection limit of 229 fg ( $10^{-9}$  M) was obtained for PA using P2-immobilized filter paper. To confirm the reusability of the fluorescent test strips, the filter papers having dark spots were rinsed with ethanol and added PA solution again. As a result, the dark spots on the filter paper faded away and then reappeared. After the third rinse, the dark spots on the filter paper could still be observed by adding PA solution at a low or high concentration (Fig. 9). These results demonstrate that the polymer-immobilized fluorescent test strips can provide a convenient and portable fluorescent platform for on-site PA detection with proper reusability and high sensitivity.

#### 4. Conclusions

In summary, two new DNDPE-based conjugated polymers P1 and P2 are synthesized and characterized. They possess good solubility, AEE feature and high photostability. Both polymers exhibit sensitive fluorescence quenching by PA. In comparison with P1, P2 displays higher

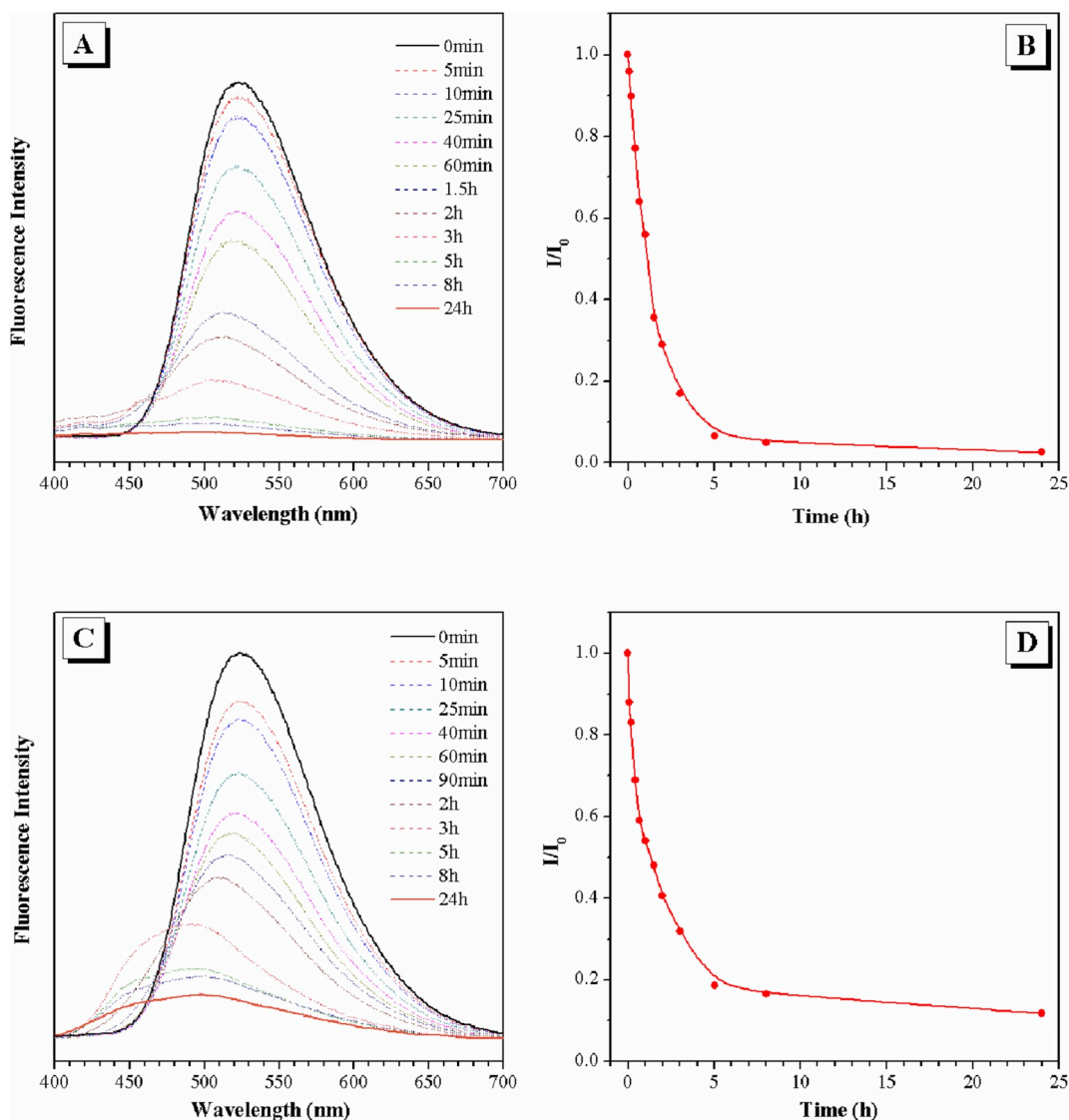


Fig. 6. (A and C) Fluorescence spectra of P1 and P2 in THF/water mixtures (P1:  $f_w = 90$  vol%; P2:  $f_w = 80$  vol%) under UV light at different exposure times. (B and D) Plots of  $I/I_0$  value versus different exposure time.  $I_0$  = fluorescence intensity at 0 min exposure time. Concentration: 0.65  $\mu$ M (P1), 0.26  $\mu$ M (P2); excitation wavelength: 350 nm.

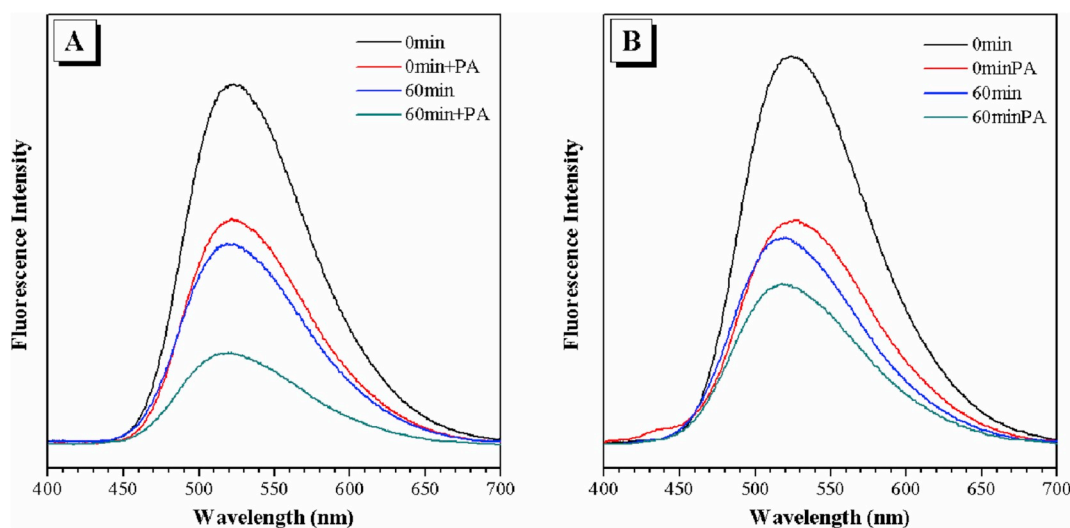


Fig. 7. (A) Fluorescence spectra of P1 in THF/water mixtures ( $f_w = 90$  vol%) at 0 min exposure time without and with PA, and at 60 min exposure time with PA, (B) Fluorescence spectra of P2 in THF/water mixtures ( $f_w = 80$  vol%) at 0 min exposure time without and with PA, and at 60 min exposure time with PA. Concentration:  $0.65 \mu\text{M}$  (P1),  $0.26 \mu\text{M}$  (P2),  $10.65 \mu\text{M}$  (PA); excitation wavelength: 350 nm.

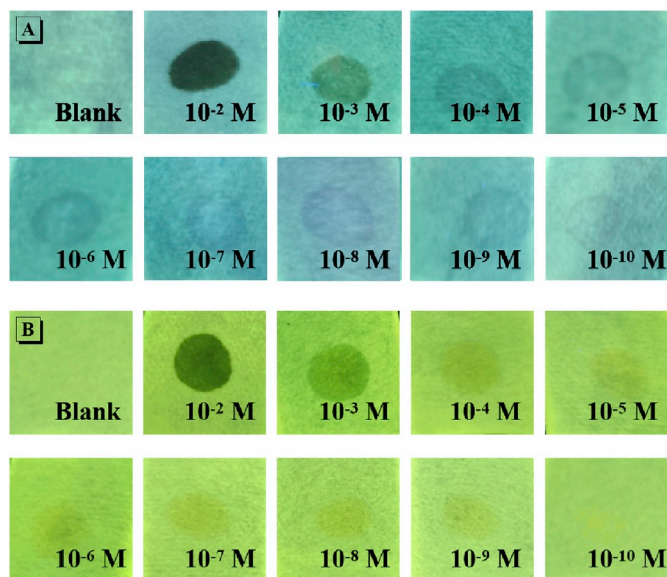


Fig. 8. Photographs of the fluorescent test strips upon the addition of PA solution at various concentrations under 365 nm UV light (A: P1, B: P2).

sensitive to PA, and the  $K_{SV}$  at the initial stage of the Stern–Volmer plots is up to  $9.8 \times 10^5 \text{ M}^{-1}$ . The sensitive detection of PA can be attributed to the existence of numerous cavities generated by the loose packing of polymer with twisted molecular conformations and high hydrophilicity. These sizeable cavities can effectively capture the PA molecules and ameliorate the PET process between polymers and PA. In addition, after exposure to UV light, these polymers still could effectively detect the PA in water. The results presented in this study hold great potential for the development of new DNDPE-based conjugated polymeric sensors for the sensitive detection of PA.

#### Declaration of competing interest

There are no conflicts of interest to declare.

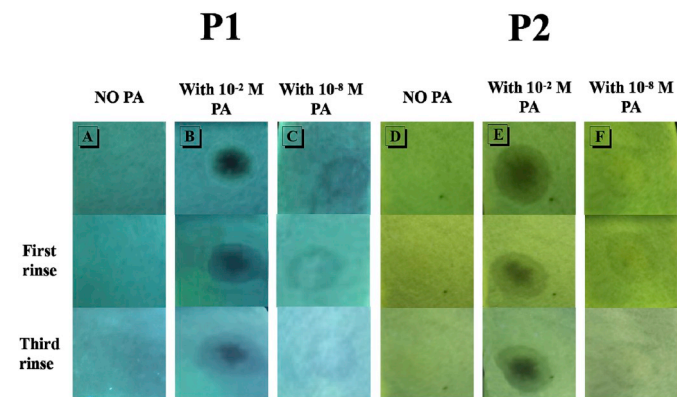


Fig. 9. Photographs of the fluorescent test strips upon the addition of PA solution at high or low concentrations under 365 nm UV light before and after rinse (P1: A, B, C; P2: D, E, F).

#### Acknowledgments

We acknowledge the financial support from the National Natural Science Foundation of China (21788102 and 21404029), National Students' Platform for Innovation and Entrepreneurship Training Program (201810346010), the Natural Science Foundation of Guangdong Province (2019B030301003).

#### References

- [1] (a) Walsh ME. Determination of nitroaromatic, nitramine, and nitrate ester explosives in soil by gas chromatography and an electron capture detector. *Talanta* 2001;54(3):427–38. (b) Mathurin JC, Faye T, Brunot A, Tabet JC. High-pressure ion source combined with an in-axis ion trap mass spectrometer. 1. instrumentation and applications. *Anal Chem* 2000;72(20):5055–62. (c) Sylvia JM, Janni JA, Klein JD, Spencer KM. Surface-enhanced Raman detection of 2,4-dinitrotoluene impurity vapor as a marker to locate landmines. *Anal Chem* 2000;72(23):5834–40. (d) Eiceman GA, Stone JA. Ion mobility spectrometers in national defense. *Anal Chem* 2004;76(21):390–7. (e) Popov IA, Chen H, Kharybin ON, Nikolaev EN, Cooks RG. Detection of explosives on solid surfaces by thermal desorption and ambient ion/molecule reactions. *Chem Commun* 2005:1953–5.
- [2] (a) Malik AH, Hussain S, Kalita A, Iyer PK. Conjugated polymer nanoparticles for the amplified detection of nitro-explosive picric acid on multiple platforms. *ACS Appl Mater Interfaces* 2015;7(48):26968–76. (b) Fu Z-H, Wang Y-W, Peng Y. Two

- fluorescein-based chemosensors for the fast detection of 2,4,6-trinitrophenol (TNP) in water. *Chem Commun* 2017;53(76):10524–7.
- [3] (a) Ashbrook PC, Houts TA. Picric acid. *Chem Health Saf* 2003;10(2):27. (b) Liu S, Luo D, Li N, Zhang W, Lei J, Li N, et al. Water-soluble nonconjugated polymer nanoparticles with strong fluorescence emission for selective and sensitive detection of nitro-explosive picric acid in aqueous medium. *ACS Appl Mater Interfaces* 2016;8(33):21700–9. (c) Toal SJ, Troglor WC. Polymer sensors for nitroaromatic explosives detection. *J Mater Chem* 2006;16(28):2871–83.
- [4] (a) Dutta P, Saikia D, Adhikary NC, Sarma NS. Macromolecular systems with MSA-Capped CdTe and CdTe/ZnS core/shell quantum dots as superselective and ultrasensitive optical sensors for picric acid explosive. *ACS Appl Mater Interfaces* 2015;7(44):24778–90. (b) Xu S, Lu H, Li J, Song X, Wang A, Chen L, et al. Dummy molecularly imprinted polymers-capped CdTe quantum dots for the fluorescent sensing of 2,4,6-trinitrotoluene. *ACS Appl Mater Interfaces* 2013;5(16):8146–54.
- [5] (a) Xie W, Zhang S-R, Du D-Y, Qin J-S, Bao S-J, Li J, et al. Stable luminescent metal-organic frameworks as dual-functional materials to encapsulate  $\text{Ln}^{3+}$  ions for white-light emission and to detect nitroaromatic explosives. *Inorg Chem* 2015;54(7):3290–6. (b) Jia X-X, Yao R-X, Zhang F-Q, Zhang X-M. A fluorescent anionic MOF with  $\text{Zn}_4(\text{trz})_2$  chain for highly selective visual sensing of contaminants: Cr (III) ion and TNP. *Inorg Chem* 2017;56(5):2690–6. (c) Deng Y, Chen N, Li Q, Wu X, Huang X, Lin Z, et al. Highly fluorescent metal-organic frameworks based on a benzene-cored tetraphenylethene derivative with the ability to detect 2,4,6-trinitrophenol in water. *Cryst Growth Des* 2017;17(6):3170–7. (d) Chen D-M, Zhang N-N, Liu C-S, Du M. Dual-emitting dye@MOF composite as a self-calibrating sensor for 2,4,6-trinitrophenol. *ACS Appl Mater Interfaces* 2017;9(29):24671–7. (e) Xing S, Bing Q, Qi H, Liu J, Bai T, Li G, et al. Rational design and functionalization of a zinc metal-organic framework for highly selective detection of 2,4,6-trinitrophenol. *ACS Appl Mater Interfaces* 2017;9(28):23828–35.
- [6] (a) Zhang Y, Shen P, He B, Luo W, Zhao Z, Tang BZ. New fluorescent through-space conjugated polymers: synthesis, optical properties and explosive detection. *Polym Chem* 2018;9(5):558–64. (b) Liu J, Zhong Y, Lam JWY, Lu P, Hong Y, Yu Y, et al. Hyperbranched conjugated polysiloles: synthesis, structure, aggregation-enhanced emission, multicolor fluorescent photopatterning, and superamplified detection of explosives. *Macromolecules* 2010;43(11):4921–36. (c) Xu B, Wu X, Li H, Tong H, Wang L. Selective detection of TNT and picric acid by conjugated polymer film sensors with donor-acceptor architecture. *Macromolecules* 2011;44(13):5089–92. (d) Wang X, Wang W, Wang Y, Sun JZ, Tang BZ. Poly(phenylene-ethynylene-alt-tetraphenylethene) copolymers: aggregation enhanced emission, induced circular dichroism, tunable surface wettability and sensitive explosive detection. *Polym Chem* 2017;8(15):2353–62.
- [7] (a) Zhang C, Zhang S, Yan Y, Xia F, Huang A, Xian Y. Highly fluorescent polyimide covalent organic nanosheets as sensing probes for the detection of 2,4,6-trinitrophenol. *ACS Appl Mater Interfaces* 2017;9(15):13415–21. (b) Rong M, Lin L, Song X, Zhao T, Zhong Y, Yan J, et al. A label-free fluorescence sensing approach for selective and sensitive detection of 2,4,6-trinitrophenol (TNP) in aqueous solution using graphitic carbon nitride nanosheets. *Anal Chem* 2015;87(2):1288–96.
- [8] (a) Bunz UH, Seehafer K, Bender M, Porz M. Poly(aryleneethynylene)s (PAE) as paradigmatic sensor cores. *Chem Soc Rev* 2015;44(13):4322–36. (b) Wu X, Li H, Xu B, Tong H, Wang L. Solution-dispersed porous hyperbranched conjugated polymer nanoparticles for fluorescent sensing of TNT with enhanced sensitivity. *Polym Chem* 2014;5(15):4521–5. (c) Jagtap SB, Potphode DD, Ghorpade TK, Palai AK, Patri M, Mishra SP. <sup>1</sup>Butyl pyrene containing poly(arylene ethynylene)s for highly sensitive and selective sensing of TNT. *Polymer* 2014;55(12):2792–8. (d) Sun X, Wang Y, Lei Y. Fluorescence based explosive detection: from mechanisms to sensory materials. *Chem Soc Rev* 2015;44(22):8019–61.
- [9] Zhou J, Chang Z, Jiang Y, He B, Du M, Lu P, et al. From tetraphenylethene to tetranaphthylethene: structural evolution in AIE luminogen continues. *Chem Commun* 2013;49(25):2491–3.
- [10] Gao M, Wu Y, Chen B, He B, Nie H, Li T, et al. Di(naphthalen-2-yl)-1,2-diphenylethene-based conjugated polymers: aggregation-enhanced emission and explosive detection. *Polym Chem* 2015;6(44):7641–5.
- [11] (a) Hong Y, Lam JWY, Tang BZ. Aggregation-induced emission. *Chem Soc Rev* 2011;40(11):5361–88. (b) Zhao Z, Lam JWY, Tang BZ. Tetraphenylethene: a versatile AIE building block for the construction of efficient luminescent materials for organic light-emitting diodes. *J Mater Chem* 2012;22(45):23726–40. (c) Cornil J, Beljonne D, Calbert J, Bredas J. Interchain interactions in organic  $\pi$ -conjugated materials: impact on electronic structure, optical response, and charge transport. *Adv Mater* 2001;13(14):1053–67.
- [12] (a) Tawfik SM, Sharipov M, Kakhkhorov S, Elmasyr MR, Lee YI. Multiple emitting amphiphilic conjugated polythiophenes-coated CdTe QDs for picogram detection of trinitrophenol Explosive and application using chitosan film and paper-based sensor coupled with smartphone. *Adv Sci* 2019;6:1801467. (b) Ganiga M, Mani NP, Cyriac J. Synthesis of organophilic carbon dots, selective screening of trinitrophenol and a comprehensive understanding of luminescence quenching mechanism. *Chemistry Select* 2018;3:4663–8. (c) Tanwar AS, Hussain S, Malik AH, Afroz MA, Iyer PK. Inner filter effect based selective detection of nitroexplosive-picric acid in aqueous solution and solid support using conjugated polymer. *ACS Sens* 2016;1:1070–7. (d) Garay R, Schvval A, Almassio M, Rosso PD, Romagnoli M, Montani R. Fluorescent amorphous distyrylnaphthalene-based polymers: synthesis, characterization and thin-film nanomolar sensing of nitroaromatics in water. *Polymers* 2018;10:1366. (e) Garay R, Rosso PGD, Romagnoli MJ, Almassio MF, Schvval AB. Photoactive thin films of terphenylene-based amorphous polymers. Synthesis, electrooptical properties, and role of photoquenching and inner filter effects in the chemosensing of nitroaromatics. *J Photochem Photobiol, A* 2019;384:112016.